

Lysophospholipid Signaling in Endothelial Dysfunction

PhD thesis

Anna Janovicz, PharmD

Doctoral School of Theoretical and Translational Medicine
Semmelweis University



Supervisors: Zoltán Benyó, MD, DSc
Éva Ruisanchez, MD, PhD

Official reviewers: Balázs Horváth, MD, PhD
Mihály Ruppert, MD, PhD

Head of the Complex Examination Committee:
György Reusz, MD, DSc

Members of the Complex Examination Committee:
Tamás Radovits, MD, PhD
Ákos Jobbágy, DSc

Budapest

2024

1. Introduction

Lysophosphatidylcholine (LPC) is a bioactive lipid, present in the plasma, that has been linked to several cardiovascular alterations, including endothelial dysfunction. In the circulation, LPC is metabolized by autotaxin (ATX), an ectoenzyme with lysophospholipase D activity that is expressed in a number of vascular cells, such as endothelial cells and macrophages. ATX cleaves the choline headgroup from the LPC molecule, generating lysophosphatidic acid (LPA), an important lysophospholipid mediator with several cellular functions. The majority of the actions of LPA are mediated by six G protein-coupled receptors, which are classified into two groups, based on their homology. LPA₁₋₃ receptors are members of the endothelial differentiation gene (EDG) family, whereas LPA₄₋₆ are known as non-EDG receptors and share similarities with purinergic receptors.

Although it has long been known that LPC contributes to the development of endothelial dysfunction by impairing the vasorelaxant properties of the vessels, its exact mechanism of action remains elusive. There are several theories for the molecular mechanism by which LPC contributes to the impairment of endothelium-dependent vasorelaxation. Many of these point to the possibility that LPC reduces the bioavailability of NO, either by uncoupling its producing enzyme, endothelial nitric oxide synthase (eNOS), or by inducing the production of reactive oxygen species (ROS) via nicotinamide adenine dinucleotide phosphate hydrogen (NOX) enzyme activation in the vascular cell. Besides, it is also possible that the LPC-evoked reduction of vasorelaxation is related to its ability to interfere with vascular cyclooxygenase (COX)-mediated pathways.

When discussing the possible mechanisms of LPC actions, it is often overlooked that LPC can be converted rapidly to LPA by the ectoenzyme ATX. Therefore, it is reasonable to hypothesize that LPC might evoke some of its effects as converted to LPA by the ATX enzyme.

2. Objectives

LPC has long been known as a pro-inflammatory mediator, disrupting the endothelium-dependent vasorelaxation, and contributing to the development of endothelial dysfunction. Despite the fact, that LPC can be metabolized to LPA by the ATX enzyme in the vasculature, the involvement of the ATX-LPA-LPA receptor axis in mediating this process has not been addressed yet. In our experiments, we aimed to investigate the involvement of the ATX-LPA-LPA receptor axis in the development of LPC-induced impairment of endothelium-dependent vasorelaxation, the downstream signaling mechanism of LPC-induced endothelial dysfunction, and the possible alterations of lysophospholipid metabolism in a mouse model of type-2 diabetes.

3. Methods

3.1. Animals

All procedures were carried out in accordance with guidelines of the Hungarian Law of Animal Protection (28/1998) and were approved by the Government Office of Pest County (PE/EA/924-7/2021). Our experiments were performed on wild-type (WT) LPA₁, LPA₂, LPA₄, and LPA₅ receptor KO, as well as COX-1 and TP receptor KO mice. Some of our experiments were performed on the BKS diabetic mouse strain. Diabetic (*Lepr^{db}/Lepr^{db}*, referred to as *db/db*) and misty (*Dock7^m/Dock7^m*, referred to as control) mice were selected for the experiments.

3.2. Preparation of thoracic aorta segments

Adult male mice were euthanized in a CO₂ chamber, followed by transcardial perfusion with Krebs solution containing 10 U/mL Heparin. The thoracic aorta was isolated and cut into 3 mm long segments and mounted on two parallel stainless-steel needles of a myograph chamber filled with 6 ml gassed Krebs solution at 37°C.

3.3. Myography

3.3.1. Examination of vasoconstrictor and vasorelaxant properties of vessels

Before every experiment, the vessels were allowed to rest for 45 min at a passive tension of 15 mN. First, the vessels were exposed to 124 mM KCl containing Krebs solution for 1 min to elicit vasoconstriction. After several washes, when the vessels returned to resting tone, phenylephrine (Phe; 10 μ M) and acetylcholine chloride (ACh; 0.1 μ M) were added to the chambers to test the smooth muscle and the endothelium function. After repeated washing, the segments were adjusted to 124 mM KCl Krebs solution for 3 min to elicit a reference maximal contraction. After washout, the vessels were pre-contracted using increasing concentrations of Phe (10 nM to 10 μ M) followed by increasing concentrations of ACh (1 nM to 10 μ M) to evoke NO-dependent vasorelaxation. In some of the experiments, to test the sensitivity of the smooth muscle to NO, sodium nitroprusside (SNP) (0.1 nmol to 10 μ mol) was administered after a stable pre-contraction elicited by Phe.

3.3.2. Examination of LPC-induced impairment of vasorelaxation

In those experiments, where we investigated the mechanism of LPC-induced endothelial dysfunction, the above-mentioned experimental protocol was followed by the administration of 124 mM KCl Krebs solution for 3 min, then, the Phe-ACh concentration-response curve (CRC) was repeated to reach the maximal responsiveness of the rings. After washout, the vessels were treated with 10 μ M 18:1 LPC for 20 min, followed by the re-administration of the Phe and ACh CRCs. In some experiments, the ATX inhibitor GLPG1690 at 10 μ M or 200 U/mL superoxide dismutase (SOD) was applied to the vessels 10 min prior to LPC administration. The superoxide scavenger Tempol (1 mM) was applied right before LPC treatment in some experiments.

3.4. Immunohistochemistry

Thoracic aorta segments, isolated from adult male WT mice, were fixed in 10% formalin for 48 hours, then embedded in paraffin and cut into 2,5 μM slices. Samples were incubated with ATX primer antibody for 16 hours. 3,3'-Diaminobenzidine reagent was used for visualization.

3.5. Quantitative real-time PCR

Whole thoracic aorta was isolated and stored at $-80\text{ }^{\circ}\text{C}$ until RNA isolation. Total RNA from the samples was extracted using Tri Reagent. Total RNA was reverse transcribed using RevertAid First Strand cDNA Synthesis kit. Quantitative real-time polymerase chain reaction (qPCR) measurements were performed on CFX Connect Real-Time PCR Detection System using SsoAdvanced Universal SYBR Green Supermix. Temperature cycles were as follows: $95\text{ }^{\circ}\text{C}$ for 60 s, $95\text{ }^{\circ}\text{C}$ for 10 s and $58\text{ }^{\circ}\text{C}$ for 30 s (40 cycles). The beta-2 microglobulin (B2m) gene was considered the housekeeping gene for normalizing gene expression. The delta–delta CT ($\Delta\Delta\text{CT}$) method was used to calculate the gene expressions of B2m, LPA₁, LPA₂, LPA₃, LPA₄, LPA₅, LPA₆ receptors, and ATX.

3.6. Amplex Red Hydrogen Peroxide Assay

Whole descending thoracic aortae were cut longitudinally and allowed to rest in 250 μL Hanks' Balanced Salt Solution (HBSS) for 60 min at $37\text{ }^{\circ}\text{C}$. To measure the basal H_2O_2 levels, the vessels were incubated with a working solution containing 50 μM Amplex Red reagent and 0,2 U/mL horseradish peroxidase (HRP) in HBSS for 15 min at $37\text{ }^{\circ}\text{C}$. The supernatant was collected and absorbance was measured at 570 nm. Then, the vessels were incubated with working solution containing 10 μM LPC for 40 min at $37\text{ }^{\circ}\text{C}$ followed by absorbance measurement of supernatant. Absorbance values were normalized to 1 min.

3.7. Measurement of serum phosphorylcholine levels

Serum phosphorylcholine level of diabetic and control mice was measured in order to examine their lipid profile. Blood samples were collected by cardiac puncture. Samples were allowed to clot for 30 min at room temperature, and centrifuged at $2000 \times g$ for 15 min at 4 °C. Serum was snap frozen for phosphorylcholine assay using a commercially available kit.

3.8. Measurement of plasma LPC levels

3.8.1. Sample preparation procedure

Lipid extracts from mouse plasma were prepared in the following way. Prior to the extraction of plasma, 10 μL lipid internal standard mixture (1,12 μM LPA 17:0, 199 μM LPC 19:0 in methanol) was added to the 100 μL plasma sample. Briefly, after vortex mixing, 2 x 600 μL of ice-cold methanol was added, followed by a vortex mixing, and the mixture was shaken for 10 minutes at room temperature. Upon 10 min of incubation at room temperature, the sample was centrifuged at 15,000 g for 15 min at 22 °C. After centrifugation, 2 x 600 μL of the upper phase was collected and dried under nitrogen at ambient temperature. For analysis, the dried extracts were dissolved in 110 μL of methanol/2-propanol/water (1/1/0.1, v/v/v%).

3.8.2. Targeted ultra-high performance liquid chromatography high-resolution mass spectrometry method

The ultra-high performance liquid chromatography high-resolution mass spectrometry (UHPLC-MS/HRMS) analysis was performed using a Waters Acquity I-Class UPLC™, equipped with a binary solvent manager, auto-sampler, and column manager. The UHPLC system was coupled to the Thermo Scientific Q Exactive Plus hybrid quadrupole-Orbitrap mass spectrometer. The UHPLC system was controlled with MassLynx V4.1 SCN 901. The control of HRMS system and HRMS data acquisition were conducted by Xcalibur™ 4.0 software. The final UHPLC-MS/HRMS method for the analysis of

LPC species was as follows: Waters Acquity UPLC HHS T3 (100 x 2.1 mm, 1.8 μ m) column with guard column, injection volume 10 μ L, and column temperature 50 °C. The mobile phase A was ammonium-formate (0.5 mM) in 60/40/1 methanol/water/formic acid (v/v/v%), and the eluent B was ammonium-formate (0.5 mM) and 1 v% formic acid in methanol. The gradient program was the following: 0 – 1 min – 10 – 10% B, 15 – 20 min – 100 – 100% B, and 20.1 – 22 min – 10% B. The flow rate was 0.4 mL/min during the analysis.

The high-resolution mass spectrometer was operated in the scheduled negative-ion parallel reaction monitoring mode using a heated electrospray ionization source with the following conditions: capillary temperature 250 °C, S-Lens RF level 50, spray voltage 2.5 kV, sheath gas flow 47.5, spare gas flow 2.25 and auxiliary gas flow 11.25, full scan with a mass range of 100-1000, isolation window 1 Da, and a resolution of 17,500. The automatic gain control setting was defined as 1×10^6 charges and the maximum injection time was set to 30 ms. The 55 eV and 25 eV of optimization energies were used for the fragmentation of LPCs.

3.10. Data Analysis

Vascular tension changes were recorded with the MP100 system and analyzed with the AcqKnowledge 3.7.3 software of Biopac System Inc. (Goleta, CA, USA). All data are presented as mean \pm SE, and 'n' indicates the number of vessels tested in myograph experiments or the number of animals tested in the case of body weight, blood glucose, H₂O₂ production, plasma LPC, and serum phosphorylcholine level measurements. In the case of the myography experiments, for each group, vessels were obtained from at least 25 three animals. Three to four aortic segments were isolated per animal. Data analysis was carried out by GraphPad Prism statistical software (version 8.0.1.244; GraphPad Software Inc., La Jolla, CA, USA). Concentration-response curves for ACh and SNP were plotted with responses expressed as percentage of the maximal contraction induced by Phe. When examining the effect of LPC on endothelial function, Two-way

ANOVA followed by Tukey's multiple comparisons test was used in order to compare the ACh concentration-response curves. When examining the vascular phenotype of db/db mice, the effects of cumulative doses of SNP and ACh were evaluated by dose-response curve fitting for the determination of Emax and EC50 values. Student's t-test or Mann-Whitney test was used when comparing two variables. $p < 0.05$ was considered statistically significant.

4. Results

We observed that in LPC-treated WT vessels the ACh-induced endothelium-dependent vasorelaxant responses were markedly attenuated (Figure 1A). To investigate the contribution of ATX to this deleterious effect of LPC, vessels were pre-treated with the selective ATX inhibitor GLPG1690. GLPG1690 significantly decreased the LPC-induced endothelial dysfunction (Figure 1A), suggesting the involvement of ATX in the effect of LPC. In order to confirm the presence of ATX on the surface of vascular cells, immunohistochemistry was used. We observed ATX is expression in all layers of the aortic tissue (Figure 1B).

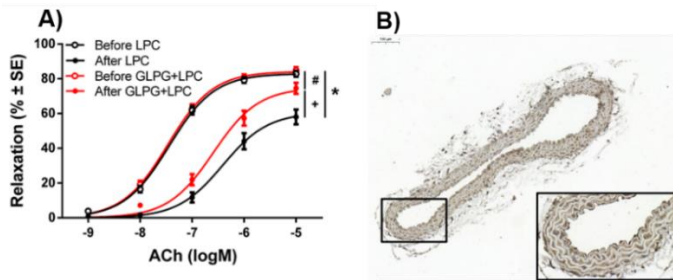


Figure 1. Involvement of ATX in LPC-induced endothelial dysfunction

Because ATX inhibition attenuated LPC-induced endothelial dysfunction, we hypothesized that it is mediated by LPA and its receptors. Therefore, the effect of LPC was tested on aorta segments isolated from knock-out (KO) mice deficient for type 1, 2, and 5 LPA receptors. In vessels of *Lpar1*, *Lpar2* and *Lpar4* KO mice, the effect of LPC was similar to that observed in wild-type (WT) animals (Figure 2A-C). On the contrary, the impairment of ACh-induced vasorelaxation by LPC was markedly attenuated in *Lpar5* KO mice (Figure 2D). These results indicate that LPC-derived LPA may contribute to the development of endothelial dysfunction through LPA₅ receptor activation.

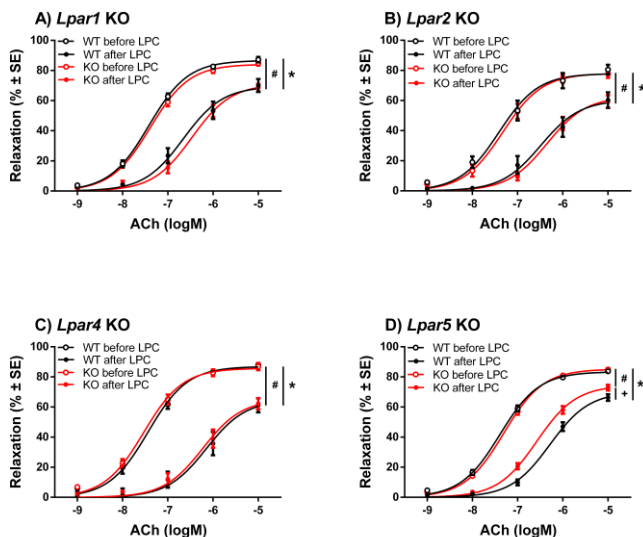


Figure 2. Involvement of LPA receptors in LPC-induced endothelial dysfunction

Next, using quantitative real-time PCR, we examined the LPA receptor and ATX expression profile of aortic tissue isolated from WT and *Lpar5* KO mice. We wanted to examine the possibility that *Lpa5* deficiency changes the expression of other LPA receptors or ATX, which could be the explanation for preserved endothelial function in *Lpar5* KO vessels. Our data showed that *Lpar5* deletion did not significantly affect the expression of LPA₁, LPA₂, LPA₃, LPA₄, LPA₆ receptors and ATX as no significant differences in mRNA expression rate were detected relative to WT. In addition, the qPCR analysis confirmed the lack of *Lpar5* in the KO mice (Figure 3).

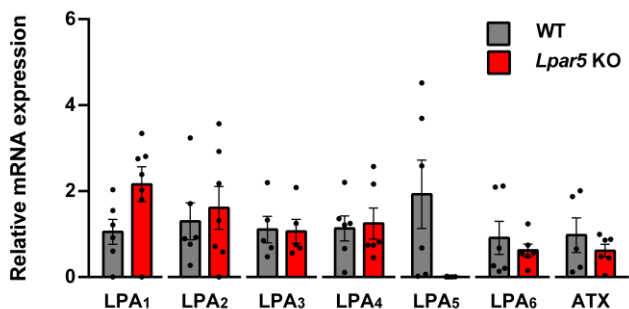


Figure 3. Expression profile of LPA receptors and ATX in WT and *Lpar5* KO aortic segments

After confirming the involvement of the ATX-LPA-LPA₅ pathway in LPC-evoked impairment of vasorelaxation, we wanted to clarify, which downstream signaling pathways mediate the LPA-dependent part of the effect. It had been reported before, that LPA can evoke COX-mediated effects, involving the release of vasoconstrictor prostanoid mediators that act on TP receptors thus as a next step, we examined the possible involvement of this pathway. We observed no significant difference in the effect of LPC in COX-1 KO (Figure 4A) and TP KO (Figure 4B) aortic segments compared to WT, suggesting that the COX-1-TP axis is not involved in this process.

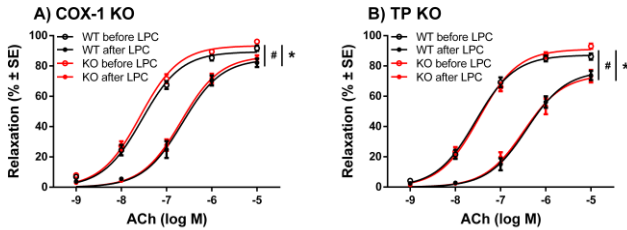


Figure 4. Involvement of COX-1 and TP in LPC-induced endothelial dysfunction

Next, we tested the effect of superoxide dismutase (SOD) on the deleterious effect of LPC. SOD prevented the effect of LPC in WT vessels (Figure 5A). Interestingly, this beneficial effect of SOD was absent in *Lpar5* KO vessels (Figure 5B). In addition, Tempol, a membrane-permeable superoxide scavenger, also failed to achieve further improvement in *Lpar5* KO vessels (Figure 5C), suggesting that LPA₅ drives ROS production. To further confirm the involvement of LPA₅ receptor in ROS generation upon LPC treatment, H₂O₂ production was determined in WT and *Lpar5* KO vessels. LPC induced a marked increase in extracellular H₂O₂ levels in aortic tissue isolated from WT mice, however, its effect was significantly ($p < 0.05$) diminished in *Lpar5* KO vessels (Figure 5D). These data suggest that the LPA₅ activation is involved in LPC-evoked ROS production.

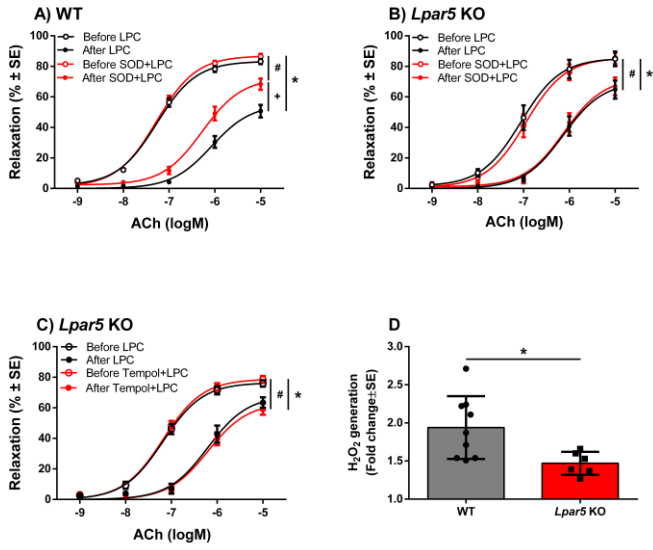


Figure 5. Involvement of ROS in LPC-induced endothelial dysfunction

In a separate study, we aimed to characterize the general metabolic and vascular phenotypes of the diabetic *db/db* mice. These animals reportedly develop obesity with elevated blood glucose levels and hyperinsulinemia. Accordingly, both the body weight (Figure 6A), and blood glucose levels were increased (Figure 6B) in *db/db* mice as compared to non-diabetic control littermates. The vessels of *db/db* animals showed marked endothelial dysfunction, as indicated by the impairment of the concentration-response relationship of ACh-induced vasorelaxation (Figure 6D). In contrast, reactivity of the vascular smooth muscle to NO remained unaltered, as there was no significant difference in the sodium nitroprusside (SNP)-induced vasorelaxation responses between the control and *db/db* mice (Figure 6E). As type 2 diabetes is associated with altered blood lipid profile, we examined the phosphorylcholine and LPC levels of control and *db/db* animals. Phosphorylcholine is the precursor of phosphatidylcholine which is an important intermediate molecule in the synthesis of several lipid mediators, including LPC. Therefore, changes in phosphorylcholine levels can be good indicators of altered lipid metabolism. Serum phosphorylcholine (Figure 6C) levels appeared to be elevated in diabetic animals, as compared to control. Next, we examined the plasma levels of the most abundant LPC species in *db/db* and control mice. All five of the studied LPCs showed a tendency for increased plasma levels in *db/db* mice, with 18:0 and 20:4 reaching the level of statistical significance (Table 1.). These results indicate that the endothelium-dependent vasoactive responses are disrupted simultaneously with the increase of serum phosphorylcholine and plasma LPC levels in a mouse model of type 2 diabetes.

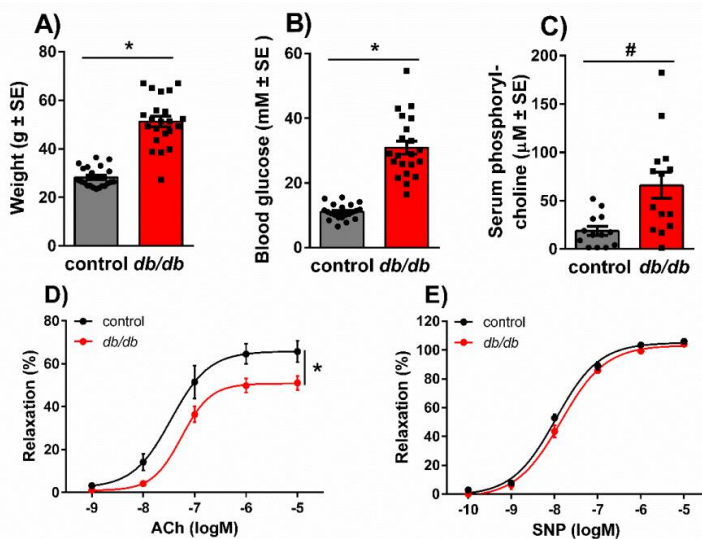


Figure 6. Metabolic and vascular phenotype of control and *db/db* diabetic mice

	Control	<i>db/db</i>	<i>p</i> value
16:0 LPC	60.51 ± 6.34 μM	73.45 ± 4.61 μM	0.11
18:0 LPC	43.19 ± 2.69 μM	56.23 ± 4.39 μM	0.03 *
18:1 LPC	16.90 ± 2.08 μM	23.81 ± 4.39 μM	0.19
18:2 LPC	42.69 ± 3.95 μM	44.91 ± 3.79 μM	0.87
20:4 LPC	1.16 ± 0.30 μM	2.48 ± 0.47 μM	0.02 *

Table 1. Plasma LPC profile of control and *db/db* mice

5. Conclusions

In our experiments, we aimed to investigate the possible involvement of ATX and LPA in the LPC-induced endothelial dysfunction and the underlying molecular mechanisms and also, to characterize the vascular and metabolic phenotype of a mouse model of diabetes. Our results indicate that:

- 18:1 LPC induces a marked impairment of ACh-evoked vasorelaxation that can be partially prevented by the inhibition of ATX enzyme implying that LPA, the product of ATX, mediates a significant part of the effect of LPC.
- LPC-derived LPA is likely to evoke its deleterious effects via LPA₅ receptor activation, as the effect of LPC was reduced in *Lpar5* KO mice. LPA₁, LPA₂ and LPA₄ are not involved in this phenomenon.
- The mRNA expression of LPA₁, LPA₂, LPA₃, LPA₄, LPA₆ and ATX do not change in the aortic tissue of *Lpar5* KO mice suggesting the other LPA receptors and ATX do not compensate for the loss of LPA₅.
- COX-1 enzyme and TP receptor are not involved in the LPC-evoked impairment of vasorelaxation, since the effect of LPC developed in COX-1 and TP receptor KO mice.
- LPC evokes ROS release from the aortic tissue of wild-type mice that is reduced in *Lpar5* KO demonstrating that LPA₅ activation by locally produced LPA results in oxidative stress contributing to endothelial dysfunction.
- Diabetic *db/db* mice present with increased serum phosphorylcholine levels, accompanied by elevated plasma levels of 18:0 and 20:4 LPC suggesting an altered blood lipid profile of diabetic animals.

6. Bibliography of the candidate's publications

Janovicz A, Majer A, Kosztelnik M, Geiszt M, Chun J, Ishii S, Tigyi GJ, Benyó Z, Ruisanchez É. Autotaxin–lysophosphatidic acid receptor 5 axis evokes endothelial dysfunction via reactive oxygen species signaling. *Experimental Biology and Medicine*. 2023;248(20):1887-1894. **IF: 3.2**

Ruisanchez É*, **Janovicz A***, Panta RC, Kiss L, Párkányi A, Straky Z, Korda D, Liliom K, Tigyi G, Benyó Z. Enhancement of Sphingomyelinase-Induced Endothelial Nitric Oxide Synthase-Mediated Vasorelaxation in a Murine Model of Type 2 Diabetes. *International Journal of Molecular Sciences*. 2023 May 6;24(9):8375) **IF: 5.6**

**Contributed equally to this work.*